

Response of the Antarctic Stratosphere to Two Types of El Niño Events

M. M. HURWITZ

NASA Postdoctoral Program, NASA Goddard Space Flight Center, Greenbelt, Maryland

P. A. NEWMAN AND L. D. OMAN

NASA Goddard Space Flight Center, Greenbelt, Maryland

A. M. MOLOD

Goddard Earth Sciences and Technology Center, University of Maryland, Baltimore County, Baltimore, Maryland

(Manuscript received 8 July 2010, in final form 6 January 2011)

ABSTRACT

This study is the first to identify a robust El Niño–Southern Oscillation (ENSO) signal in the Antarctic stratosphere. El Niño events between 1979 and 2009 are classified as either conventional “cold tongue” events (positive SST anomalies in the Niño-3 region) or “warm pool” events (positive SST anomalies in the Niño-4 region). The 40-yr ECMWF Re-Analysis (ERA-40), NCEP, and Modern Era Retrospective–Analysis for Research and Applications (MERRA) meteorological reanalyses are used to show that the Southern Hemisphere stratosphere responds differently to these two types of El Niño events. Consistent with previous studies, cold tongue events do not impact temperatures in the Antarctic stratosphere. During warm pool El Niño events, the poleward extension and increased strength of the South Pacific convergence zone favor an enhancement of planetary wave activity during September–November. On average, these conditions lead to higher polar stratospheric temperatures and a weakening of the Antarctic polar jet in November and December, as compared with neutral ENSO years. The phase of the quasi-biennial oscillation (QBO) modulates the stratospheric response to warm pool El Niño events; the strongest planetary wave driving events are coincident with the easterly phase of the QBO.

1. Introduction

El Niño–Southern Oscillation (ENSO) has a stratospheric signature in both the tropics and in the Arctic. In the tropics, the lower-stratospheric temperature response to ENSO is opposite in sign to that in the troposphere; that is, a cooling associated with ENSO warm phase (El Niño) events (Calvo Fernandez et al. 2004; García-Herrera et al. 2006; Free and Seidel 2009). This upper-tropospheric warming and lower-stratospheric cooling reflects a strengthened tropical upwelling (Calvo et al. 2010). Using both observations and a chemistry–climate model (CCM), Randel et al. (2009) showed that increased tropical upwelling during El Niño events leads to coherent variability in tropical ozone and temperature.

El Niño events have been shown to weaken the Northern Hemisphere polar vortex. El Niño–related warming of the Arctic stratosphere has been identified in observational (Bronnimann et al. 2004; Free and Seidel 2009) and modeling studies (Sassi et al. 2004; Manzini et al. 2006; Cagnazzo et al. 2009). Warming of the Arctic stratosphere is a response to increased planetary wave driving; Garfinkel and Hartmann (2008) showed that the extratropical tropospheric teleconnections produced during El Niño events weaken the Arctic vortex, leading to higher stratospheric temperatures during the NH winter season. The phase of the quasi-biennial oscillation (QBO) (Garfinkel and Hartmann 2007; Bronnimann 2007) and volcanic activity (Randel et al. 2009) modulate this response. The Arctic vortex is weakest in years when El Niño events coincide with the easterly phase of the QBO (Garfinkel and Hartmann 2007).

Previous studies of the stratospheric response to ENSO have considered a single type of El Niño event. The sea surface temperature anomaly pattern associated

Corresponding author address: M. M. Hurwitz, NASA Goddard Space Flight Center, Code 613.3, Greenbelt, MD 20771.
E-mail: margaret.m.hurwitz@nasa.gov

with these events, a band of positive SST anomalies spanning the eastern Pacific, was identified by Rasmusson and Carpenter (1982) and was termed a “cold tongue” El Niño event (hereafter CT El Niño) by Kug et al. (2009). The SST and precipitation anomalies associated with CT El Niño events develop during the June–August (JJA) and September–November (SON) seasons, peak in December–February (DJF), and decay in the March–May (MAM) season. The multivariate ENSO index (MEI) (www.esrl.noaa.gov/psd/people/klaus.wolter/MEI) and Niño-3 and Niño-3.4 indices (www.cpc.noaa.gov/data/indices) capture this leading mode of variability in the tropical Pacific (Calvo Fernandez et al. 2004; Ashok et al. 2007) and maximize during CT El Niño events, when SST anomalies and convective activity in the eastern equatorial Pacific are unusually high. The two largest CT El Niño events of the satellite era occurred in 1982/83 and 1997/98 (Kug et al. 2009).

Recent literature recognizes a second type of El Niño event. These events have been referred to as “dateline El Niño” (Larkin and Harrison 2005), “El Niño Modoki” (Ashok et al. 2007), and “warm pool” El Niño (Kug et al. 2009) (hereafter WP El Niño). WP El Niño events capture the secondary mode of variability in tropical Pacific SSTs: positive SST anomalies in the tropical central Pacific and negative SST anomalies in the tropical western Pacific and subtropical central Pacific (Ashok et al. 2007). SST and precipitation anomalies maximize during the SON and DJF seasons (Kug et al. 2009; Yu and Kim 2010). The largest observed WP El Niño events occurred in the early 1990s.

The two types of El Niño events can be distinguished not only by the region in which SST anomalies are greatest, but also by the relative position and strength of the South Pacific convergence zone (SPCZ). Vera et al. (2004) found that the extratropical component of the SPCZ is stronger and extends farther south in WP El Niño-like events as compared with either CT El Niño-like or ENSO neutral events. The same authors found a relative increase in planetary wave activity in the south central Pacific in response to all El Niño events, and, furthermore, identified a Rossby wave source region centered at approximately 20°S, 240°E in El Niño events with enhanced SPCZ activity (WP El Niño-like) relative to El Niño events with suppressed SPCZ activity (CT El Niño-like).

While the planetary wave response to CT El Niño modulates conditions in the Arctic stratosphere (Garfinkel and Hartmann 2008), this paper shows that analogous enhancements in wave activity during recent WP El Niño events affected conditions in the Antarctic stratosphere. In particular, differences between the SH wave response to WP El Niño and CT El Niño are consistent with differences in the strength of the Antarctic vortex during

these two types of El Niño events. In section 2, atmospheric datasets are defined and El Niño events are categorized. In section 3, tropospheric stationary wave patterns, eddy heat flux, stratospheric temperature, and winds are used to illustrate the atmospheric response to El Niño events, as well as the modulation of this response by the QBO. Section 4 provides a summary of the results and a brief discussion.

2. Methods

a. Identification of El Niño events and QBO phase

In this study, El Niño events are identified using two climate indices. The Niño-3 index (www.cpc.noaa.gov/data/indices) measures SST anomalies in the eastern equatorial Pacific Ocean (the Niño-3 region: 5°S–5°N, 210°–270°E). The Niño-4 index measures SST anomalies in the central equatorial Pacific Ocean (the Niño-4 region: 5°S–5°N, 160°–210°E). In this study, CT El Niño events are identified when SON-mean Niño-3 anomalies exceed one standard deviation from the 1971–2000 mean (Fig. 1b).

WP El Niño events are identified when SON seasonal-mean Niño-4 anomalies exceed one standard deviation from the 1971–2000 mean and are larger than the corresponding Niño-3 anomalies (Fig. 1a). Note that WP El Niño events appear as secondary peaks in the Niño-3 time series. Note also that the Niño-3 standard deviation is larger than the Niño-4 standard deviation; that is, the magnitudes of the positive SST anomalies that define a WP El Niño event are smaller than those that define a CT El Niño event. Kug et al. (2009) used the SON – DJF seasonal mean to select a slightly different set of WP and CT El Niño events; also, the authors defined a “mixed” type of El Niño event in which the maximum area of SST anomalies is located between the Niño-3 and Niño-4 regions.

Neutral ENSO years are defined as those when the SON and DJF mean Niño-3 and Niño-4 indices are both between -0.7 and 0.7 . Table 1 specifies years in which the above criteria are met. Figure 2 shows SST differences between the two types of El Niño events and the set of ENSO neutral years; SST composites are formed from the Hadley Centre Global Sea Ice and Sea Surface Temperature (HadISST1) dataset (Rayner et al. 2003).

A third index characterizes the phase of the quasi-biennial oscillation (QBO). This index is calculated by averaging 50-hPa zonal winds between 10°S and 10°N in November and December of each year. QBO easterly years (QBO-E) are defined when the QBO index is larger than 2 m s^{-1} and QBO westerly years (QBO-W) are defined when the QBO index is less than -2 m s^{-1} (Fig. 1c). Easterly QBO years are denoted with asterisks

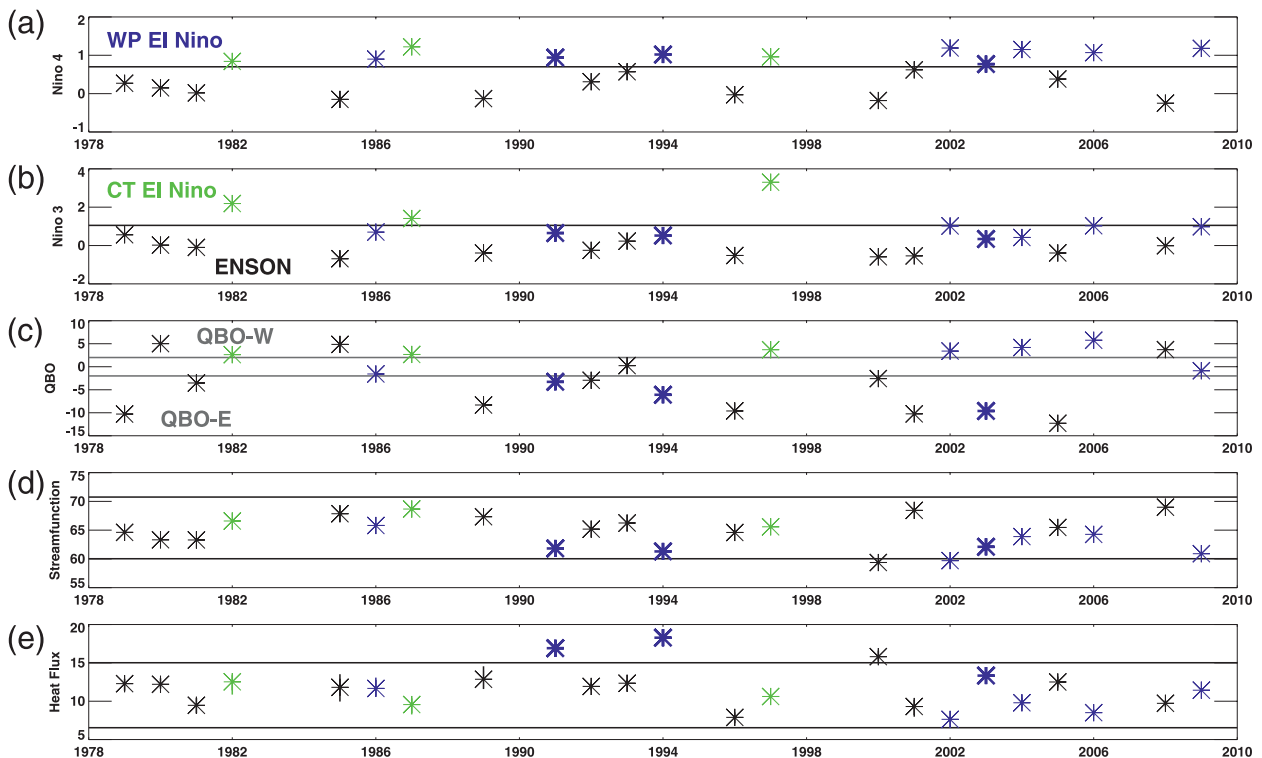


FIG. 1. Time series showing conditions during El Niño and ENSO neutral events during the 1979–2009 period. Thick (thin) blue stars indicate WP El Niño events coincident with the easterly (westerly or neutral) phase of the QBO. Green stars indicate CT El Niño events. Black stars indicate ENSO neutral events. (a) SON Niño-4 index (as described in the text); the black horizontal line shows the cutoff value defining WP El Niño events. (b) SON Niño-3 index; the black line shows the cutoff value defining CT El Niño events. (c) QBO index (as described in the text); gray lines show the cutoff values defining easterly QBO and westerly QBO events. (d) Average SON streamfunction in the region 55° – 75° S, 210° – 270° E (10^{-6} $\text{m}^3 \text{s}^{-1}$); black lines indicate ± 2 standard deviations from the mean of ENSO neutral events. (e) October–November eddy heat flux magnitude (K m s^{-1}) at 100 hPa, 40° – 80° S; black lines indicate ± 2 standard deviations from the mean of ENSO neutral events. The QBO, streamfunction, and eddy heat flux diagnostics are based on the NCEP reanalysis.

in Table 1; years when WP El Niño coincides with the easterly phase of the QBO are denoted as thick blue stars in Fig. 1c. Note that tropical Pacific SSTs in WP El Niño and QBO-E years (Fig. 2a) are not significantly different from SSTs in WP El Niño events coincident with a neutral or westerly QBO (Fig. 2b).

b. Atmospheric datasets

Various atmospheric datasets are used to assess the atmospheric response to the two types of El Niño events as defined in section 2a. Monthly mean precipitation is taken from the Global Precipitation Climatology Project (GPCP) merged precipitation dataset, version 2.1 (Adler et al. 2003; Bolvin et al. 2009). Data are available from 1979 through 2007, with $2.5^{\circ} \times 2.5^{\circ}$ horizontal resolution. Three meteorological reanalyses are used to calculate streamfunction, heat flux, temperature, and zonal wind diagnostics. Despite the small number of El Niño events included in this analysis, similarities in the El Niño response in multiple reanalysis datasets help identify

robust results. Also, multiple reanalyses test the sensitivity of the results to the number and type of events included in the analysis.

The 40-yr European Centre for Medium-Range Weather Forecasts Re-Analysis (ERA-40) (Uppala et al. 2005) has vertical coverage up to 1 hPa and, for this study, is interpolated to a $2.5^{\circ} \times 2.5^{\circ}$ horizontal grid. The 1979–2001 period is used in this analysis.

The Modern Era Retrospective–Analysis for Research and Applications (MERRA) is a reanalysis dataset based on an extensive set of satellite observations and on the Goddard Earth Observing System, version 5 (GEOS 5) data analysis (Bosilovich 2008). Currently, the MERRA reanalysis extends from 1979 through 2009. The MERRA reanalysis has vertical coverage up to 0.1 hPa and for this study has $1.25^{\circ} \times 1.25^{\circ}$ horizontal resolution.

The National Centers for Environmental Prediction (NCEP)–U.S. Department of Energy (DOE) reanalysis product (Kanamitsu et al. 2002) covers the period from

TABLE 1. Years classified as WP El Niño (WPEN), CT El Niño (CTEN), and ENSO neutral (ENSON). Classification is based on the SON mean Niño-3 and Niño-4 indices, as described in the text. Events marked with an asterisk coincide with years when the QBO is in its easterly phase, using a QBO index based on zonal winds from the NCEP reanalysis.

WPEN	1986, 1991*, 1994*, 2002, 2003*, 2004, 2006, 2009
CTEN	1982, 1987, 1997
ENSON	1979*, 1980, 1981*, 1985, 1989*, 1992*, 1993, 1996*, 2000*, 2001*, 2005*, 2008

1979 through 2009. The NCEP reanalysis has $2.5^\circ \times 2.5^\circ$ horizontal resolution and vertical coverage up to 10 hPa.

3. Results

a. Southern Hemisphere response to WP El Niño and CT El Niño events

In this section, observed precipitation, horizontal winds, eddy heat flux, and temperature fields are used to show that the strength and position of the SPCZ control the SH stratospheric response to El Niño events.

The strength and position of the SPCZ are largely controlled by the phase of ENSO (Juillet-Leclerc et al. 2006) and by the type of El Niño event. Figure 3 shows GPCP precipitation differences in WP El Niño and CT El Niño events, relative to an ENSO neutral composite, in the SPCZ region. There is more precipitation associated with the SPCZ, which extends diagonally from the northwest to the southeast corner of each plot, during both types of El Niño events than in ENSO neutral years. In WP El Niño events (Fig. 3a) there is a coherent increase in precipitation of $0.5\text{--}1 \text{ mm day}^{-1}$ at the southeastern edge of the SPCZ. This region of increased precipitation

coincides with the location of the largest correlations between precipitation and October–November midlatitude heat flux at 100 hPa (Fig. 4).

El Niño events trigger a planetary wave response in the SH. Vera et al. (2004) found that the intensification and southeastward extension of SPCZ activity strengthened the local overturning circulation, leading to a relative Rossby wave source in the south central Pacific in WP-like as compared with CT-like El Niño events. This analysis will reproduce the results of Vera et al. using WP and CT El Niño events, as defined in section 2a. In Fig. 5, 250-hPa SON streamfunction differences from the ENSO neutral composite illustrate the planetary wave responses to both types of El Niño events. Each panel of Fig. 5 shows a wave train response to El Niño: negative streamfunction differences in the subtropics, close to the date line (region A in Fig. 4c); positive streamfunction differences at midlatitudes (region B); and negative streamfunction differences around $60^\circ\text{S}, 240^\circ\text{E}$ (region C). The red arrows in Figs. 5a and 5b indicate the approximate propagation direction of the wave trains. The region A and B differences are statistically significant in both types of El Niño events and in all three reanalyses. Region C differences are statistically significant in the case of WP El Niño (Figs. 5a,c,e) but not in CT El Niño (Figs. 5b,d,f). Figure 1d shows a time series of 250-hPa streamfunction in region C; note that the lowest values are concurrent with WP El Niño events. This evidence suggests that there is a stronger planetary wave response to WP El Niño events than to CT El Niño events, consistent with Vera et al. (2004).

Eddy heat flux is used to quantify the amount of planetary wave energy entering the stratosphere during El Niño and ENSO neutral events. Eddy heat flux ($\overline{v'T'}$) at 100 hPa averaged between 40° and 80°S has been used to diagnose planetary wave driving in chemistry–climate model validation studies (Austin et al. 2003; Eyring et al.

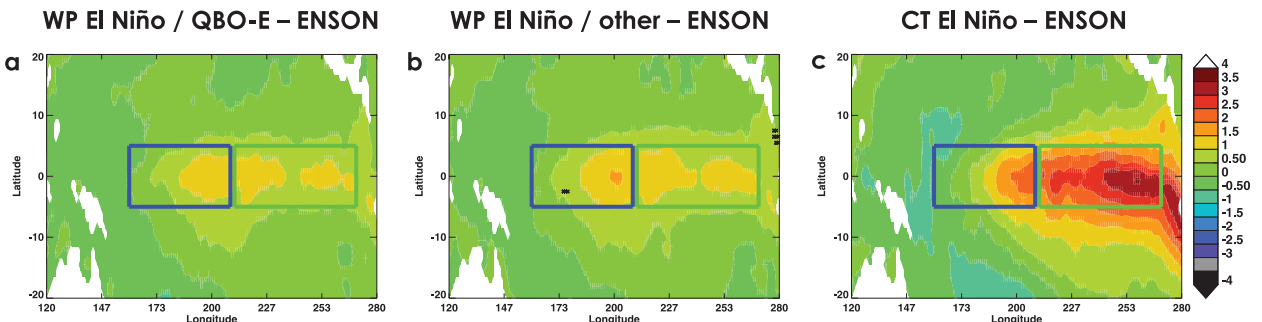


FIG. 2. HadISST1 SST differences (K) from a composite of ENSO neutral events, averaged from September through February, in (a) WP El Niño events with easterly QBO, (b) WP El Niño events with neutral or westerly QBO, and (c) CT El Niño events. The Niño-3 and Niño-4 regions are indicated by the green and blue boxes, respectively. Black crosses in (b) indicate regions where SST differences between WP El Niño events with easterly QBO and WP El Niño events with neutral or westerly QBO are significant at the 95% confidence level.

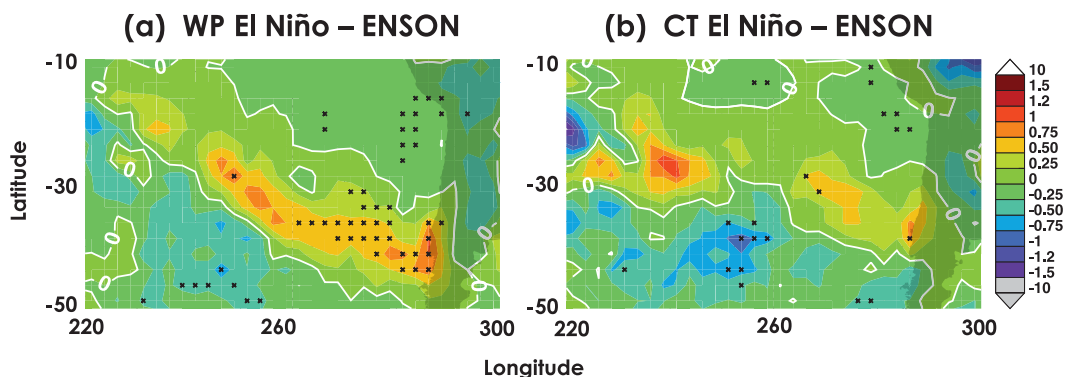


FIG. 3. GPCP SON precipitation differences (mm day^{-1}) from a composite of ENSO neutral events, in (a) WP and (b) CT El Niño events, in the SPCZ region during the 1979–2007 period. White contours indicate zero difference from the composite of ENSO neutral events. Black crosses indicate differences significant at the 95% confidence level.

2006). October–November eddy heat flux at 100 hPa will be the focus of this study, as previous work has shown that it plays an important role in the timing of the breakup of the Antarctic vortex (Hurwitz et al. 2010). Table 2 shows the mean eddy heat flux magnitudes in each of the ENSO cases and for each of the reanalyses. For the MERRA and NCEP reanalyses, mean eddy heat flux is shown both for the ERA-40 period (1979–2001) and for 1979–2009. Eddy heat flux values are broadly consistent among the three reanalyses (see also Fig. 1e) and are not sensitive to the length of the time series used in the analysis. Note, however, that eddy heat flux is largest in the WP El Niño cases and larger during the 1979–2001 period than during the 1979–2009 period. Variability among WP El Niño events is roughly twice as

large as that between CT El Niño and ENSO neutral events (see discussion in section 3b).

Newman et al. (2001) identified a positive relationship between midlatitude eddy heat flux at 100 hPa and polar temperatures at 50 hPa, with roughly a one-month lag. Given the relatively larger October–November eddy heat flux values in WP El Niño events as compared to CT El Niño and ENSO neutral events (Table 2), the November–December stratospheric temperature response to WP El Niño events would be expected to be larger than that of CT El Niño events. Figure 6 shows mean November–December temperature differences in the WP and CT El Niño composites, as compared with neutral ENSO years. At polar latitudes, WP El Niño events (Figs. 6a,c,e) warm the tropical upper troposphere and

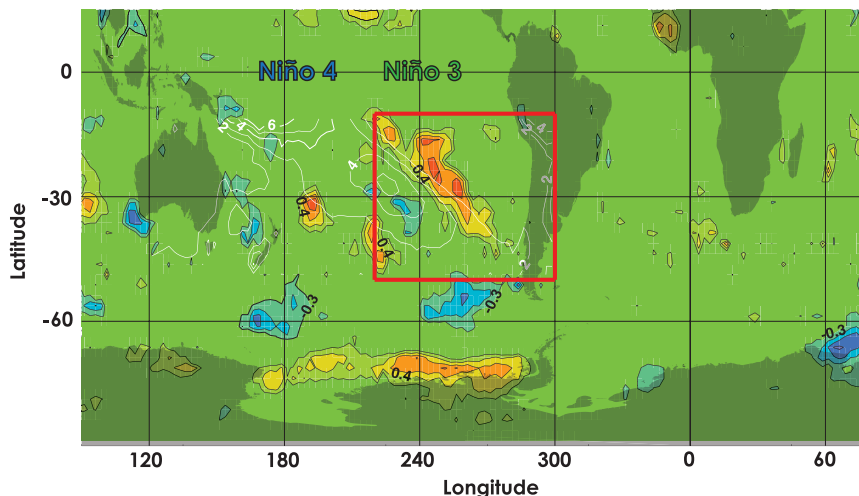


FIG. 4. Filled contours show the point correlation between GPCP SON precipitation and NCEP October–November eddy heat flux at 100 hPa, 40° – 80° S for the 1979–2007 period. The highest correlation coefficient is 0.69. The SPCZ region, highlighted in Fig. 3, is shown as the red box. White contours show climatological mean SON precipitation (mm day^{-1}) in the South Pacific. The locations of the Niño-3 and Niño-4 regions are labeled.

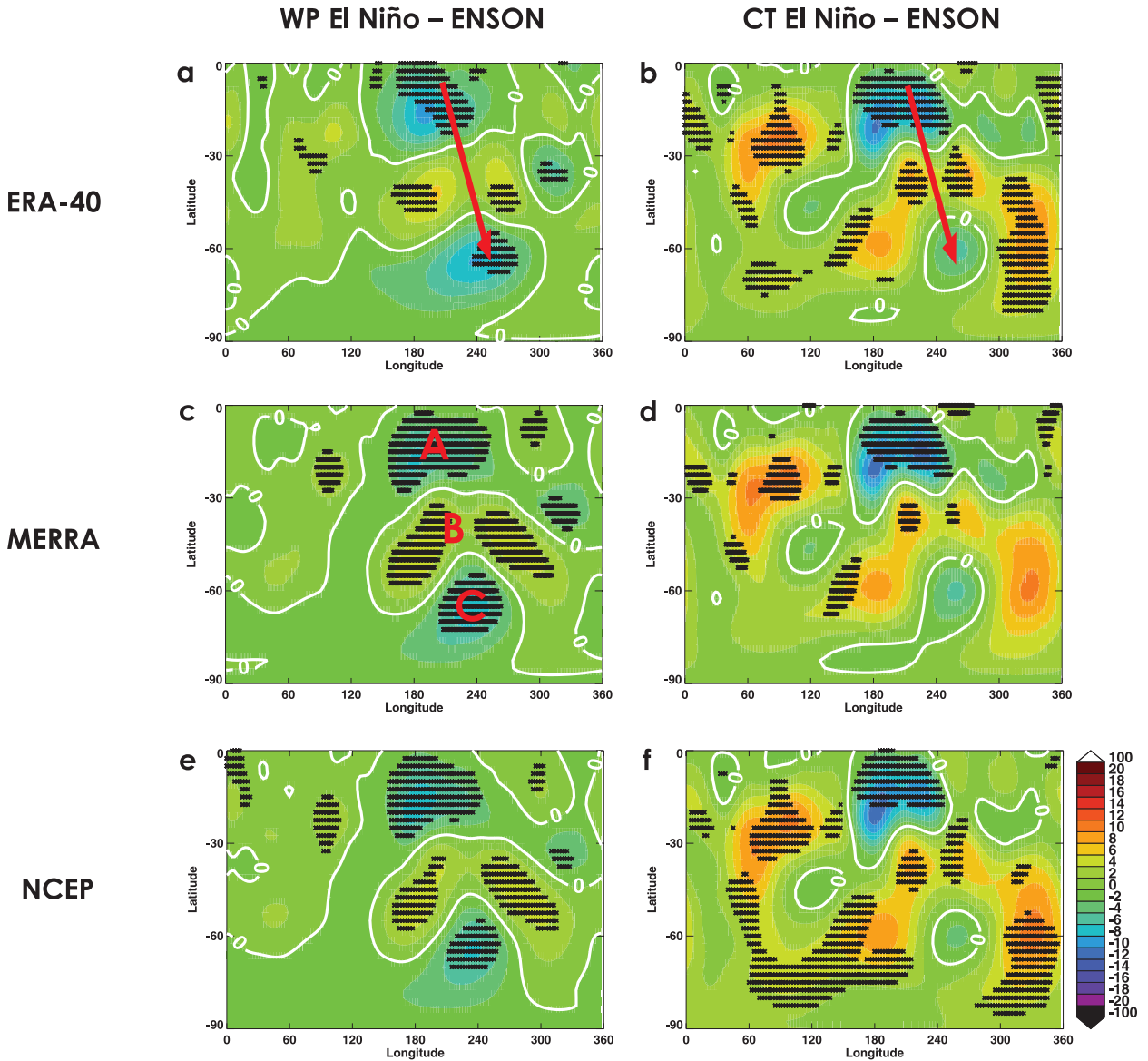


FIG. 5. Longitude–latitude contour plots showing SON mean 250-hPa streamfunction differences ($10^{-6} \text{ m}^3 \text{ s}^{-1}$), from a composite of ENSO neutral events in (a),(c),(e) WP El Niño events and (b),(d),(f) CT El Niño events. The ERA-40 reanalysis is shown for the 1979–2001 period, while the MERRA and NCEP reanalyses are shown for the 1979–2009 period. White contours indicate zero difference from the composite of ENSO neutral events. Black crosses indicate differences significant at the 95% confidence level. Red arrows in (a) and (b) indicate the approximate propagation direction of the planetary wave trains induced by El Niño events. Red letters A, B, and C in (c) indicate the three regions discussed in the text.

lower stratosphere and cool the upper stratosphere. The lower stratospheric warming response is statistically significant in ERA-40 (3–5 K) but not in MERRA or NCEP. The upper stratospheric cooling (1–2 K in MERRA, see Fig. 6c) is a wave filtering effect (Hurwitz et al. 2010): in WP El Niño events heat flux is higher and the Antarctic vortex breaks up earlier. Summertime easterly winds do not allow planetary wave propagation, leading to lower temperatures. During CT El Niño events (Figs. 6b,d,f), consistent with previous observational

studies (Free and Seidel 2009; Randel et al. 2009), none of the reanalyses shows a statistically significant temperature response in the Antarctic lower stratosphere.

b. QBO influence on the response to WP El Niño events

The response of the Antarctic stratosphere to WP El Niño events is systematically different from that to CT El Niño events. However, the relative increases in

TABLE 2. October–November mean eddy heat flux magnitude (K m s^{-1}) at 40° – 80°S , 100 hPa ± 2 standard deviations for the WP El Niño, CT El Niño, and ENSO neutral cases. Years shown in the second row denote SON seasons.

	ERA-40	MERRA		NCEP	
	1979–2001	1979–2001	1979–2009	1979–2001	1979–2009
WPEN	16.55 ± 6.18	15.77 ± 8.02	12.47 ± 7.74	14.54 ± 6.76	11.58 ± 7.06
CTEN	11.41 ± 3.44	11.36 ± 3.48	11.36 ± 3.48	9.93 ± 2.88	9.93 ± 2.88
ENSON	12.22 ± 5.18	11.73 ± 4.12	11.72 ± 3.94	10.82 ± 4.52	10.78 ± 4.24

heat flux and polar lower stratospheric temperatures during WP El Niño events are not statistically different from ENSO neutral events. The high degree of variability among WP El Niño events may be related to the phase of the QBO.

In the Arctic lower stratosphere the largest warming response to CT El Niño is seen in years when the phase of the QBO is easterly (Calvo Fernandez et al. 2004; Manzini et al. 2006). The Antarctic lower stratosphere responds analogously. Of WP El Niño events, the eddy heat flux magnitude is larger in years when the QBO is easterly than in years when winds are either weak or westerly (Table 3); differences between the two QBO groupings are significant at the 95% level in all three reanalyses. Conversely, in ENSO neutral years the QBO phase makes no difference to the magnitude of the October–November eddy heat flux. The sensitivity of CT El Niño events to QBO phase cannot be assessed, as all three observed CT El Niño events coincide with weak equatorial zonal winds at 50 hPa.

The NCEP reanalysis is used to examine the temperature response to WP El Niño events as a function of QBO phase, as its time series are long enough to sample of each of the QBO and ENSO cases. The MERRA reanalysis yields very similar results. Figures 7a and 7b show temperature differences between WP El Niño events, partitioned by QBO phase, and the ENSO neutral composite. At high latitudes a warming of 3–5 K is seen in easterly QBO years (Fig. 7a), whereas there is no significant warming in years when the QBO is either neutral or westerly (Fig. 7b).

In the Antarctic stratosphere the zonal wind response to El Niño events is consistent with the temperature response. The relative warming of the lower Antarctic stratosphere during WP El Niño events reduces the meridional temperature gradient and, by the thermal wind balance, weakens the polar jet. The largest wind differences from the ENSO neutral composite are seen in WP El Niño events coincident with QBO-E (note the easterly winds at 50 hPa at the equator in Fig. 7c). In the NCEP reanalysis, there are statistically significant negative zonal wind differences of up to 7 m s^{-1} in the lower and middle stratosphere at $\sim 60^{\circ}\text{S}$ (Fig. 7c). This jet weakening is approximately twice as large as that seen in the Whole

Atmosphere Community Climate Model in the Arctic stratosphere in January (Taguchi 2010) in the ENSO warm phase as compared with cold phase events. Consistent with the negligible temperature differences seen in Fig. 6, the Antarctic jet does not weaken in response to CT El Niño events.

4. Summary and discussion

This study examined the response of the Antarctic stratosphere to two types of El Niño events: warm pool (WP) El Niño and cold tongue (CT) El Niño. WP El Niño events are characterized by positive SST anomalies in the equatorial central Pacific (i.e., the Niño-4 region) during austral spring and summer. This analysis found that, for the 1979–2009 period, the Niño-4 index is a better indicator of the SH dynamical response to El Niño than are indices that favor the eastern Pacific. The Niño-3, Niño-3.4, and MEI indices have been used in previous studies to identify the stratospheric signature of CT El Niño events in the tropics and in the Arctic; however, these indices have failed to identify an El Niño response in the Antarctic stratosphere. Thus, evaluation of the global impact of ENSO on the stratosphere requires measures of SST changes in both the eastern (Niño-3) and central equatorial Pacific (Niño-4) regions.

The strength and poleward extension of the SPCZ during the SON season largely determine the SH stratospheric response to ENSO. While SPCZ activity increases during both types of El Niño events, precipitation is significantly enhanced in the southeastern part of the SPCZ during WP El Niño events. Both types of El Niño events generated a planetary wave response in the SH troposphere, but this wave response extended farther poleward during WP El Niño events than during CT El Niño events. As a result, the SH planetary wave driving in October and November (specifically, the midlatitude eddy heat flux at 100 hPa) was stronger during WP El Niño events, compared with both CT El Niño events and ENSO neutral years.

During WP El Niño events, enhanced planetary wave activity warmed the Antarctic upper troposphere and lower stratosphere and weakened the stratospheric polar jet. The Antarctic response to WP El Niño appears

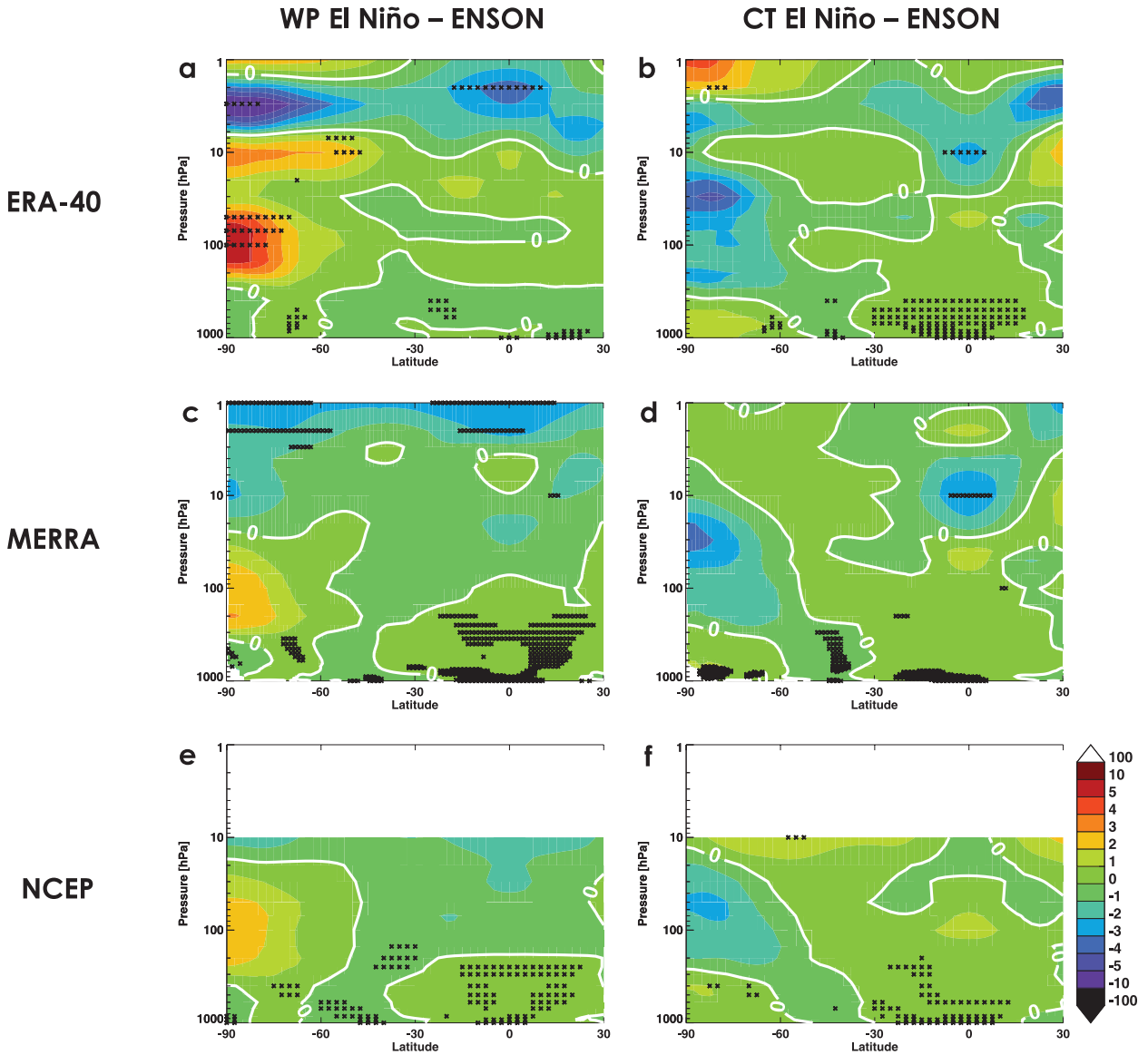


FIG. 6. Latitude–height cross sections of November–December mean temperature differences (K), from a composite of ENSO neutral events, in (a),(c),(e) WP El Niño events and (b),(d),(f) CT El Niño events. The ERA-40 reanalysis is shown for the 1979–2001 period, while the MERRA and NCEP reanalyses are shown for the 1979–2009 period. White contours indicate zero difference from the composite of ENSO neutral events. Black crosses indicate differences that are significant at the 95% confidence level.

to be modulated by the phase of the QBO: a 3–5-K warming was seen in QBO easterly phase events whereas there was no significant warming in years with a weak or westerly QBO. Following the Holton and Tan (1980) mechanism, the easterly phase of the QBO may confine lower stratospheric planetary wave breaking to middle and high latitudes, weakening the Antarctic vortex. However, during WP El Niño events the strength of the SPCZ is highly dependent on the phase of the QBO, suggesting that a tropical mechanism may be involved. Collimore et al. (2003) argue that the phase of the QBO

modulates the tropopause height and thus the height of deep convection in the tropics. These authors found a strengthening of convective activity in the SPCZ region during austral spring in QBO-E relative to QBO-W years, possibly explaining the QBO modulation of the SH stratospheric response to WP El Niño events. Relative to the 2–4-K warming of the Arctic lower stratosphere during CT El Niño events, as found by Free and Seidel (2009), the warming of the Antarctic lower stratosphere during WP El Niño events was comparable during easterly QBO years but weaker on average. Coupled

TABLE 3. October–November mean eddy heat flux magnitude (K m s^{-1}) at 40° – 80°S , 100 hPa ± 2 standard deviations for the WP El Niño and ENSO neutral cases, and as a function of QBO phase.

		ERA-40	MERRA	NCEP
WPEN	QBO-E	18.28 ± 2.06	16.64 ± 5.10	15.26 ± 4.34
	QBO-W and neutral	13.08	9.97 ± 2.94	8.90 ± 2.58
ENSON	QBO-E	11.90 ± 6.78	11.73 ± 5.06	10.62 ± 5.72
	QBO-W and neutral	12.68 ± 1.28	11.71 ± 2.08	11.00 ± 2.58

ocean–atmosphere model simulations predict that the pattern of SST trends will favor WP El Niño events in the future (Yeh et al. 2009; Xie et al. 2010); thus, ENSO-related warming of the Antarctic lower stratosphere may offset some of the direct radiative cooling by greenhouse gases.

While WP El Niño events have a significant impact on temperature, they have a negligible impact on polar ozone. WP El Niño events reach maturity in austral spring and summer (Kug et al. 2009), after the formation of the ozone hole. Compared with ENSO neutral years, ozone differences in the Antarctic lower stratosphere were negligible in both WP El Niño and CT El Niño events.

The ERA-40, MERRA, and NCEP reanalyses were in agreement when the same time periods were compared.

That is, neither the different observational datasets used to form the three reanalyses nor their different horizontal and vertical resolutions affected the results. However, the stratospheric response to WP El Niño events was dependent on the time period analyzed: the WP El Niño events after 2001 mainly occurred in westerly or neutral QBO years, weakening the mean temperature response to WP El Niño events in MERRA and NCEP (1979–2009) as compared with ERA-40 (1979–2001).

One shortcoming of using meteorological reanalyses to diagnose the stratospheric response to El Niño events is the small number of such events that occurred between 1979 and 2009. In particular, whereas the temperature and zonal wind responses were statistically robust and multiple reanalysis datasets yielded consistent results, the WP

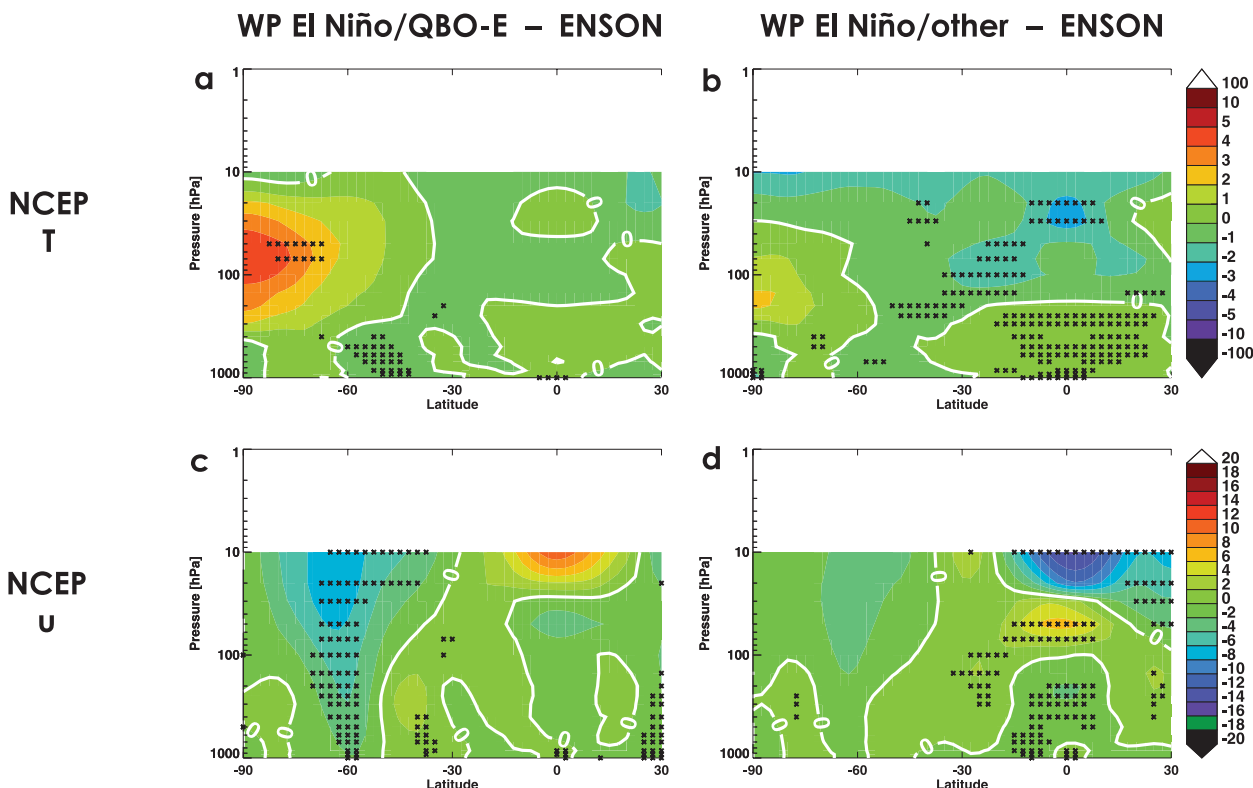


FIG. 7. Latitude–height cross sections of November–December (a),(b) mean temperature differences (K) and (c),(d) zonal wind differences (m s^{-1}) from a composite of ENSO neutral events, in WP El Niño events with (a),(c) easterly QBO and (b),(d) neutral or westerly QBO. The NCEP reanalysis is shown for the 1979–2009 period. White contours indicate zero difference from the composite of ENSO neutral events. Black crosses indicate differences that are significant at the 95% confidence level.

El Niño and easterly QBO composite consisted of just three events. Time-slice simulations, with repeating El Niño-like boundary conditions, would greatly increase the sample size and better separate the WP El Niño, CT El Niño, and QBO signals from the variability between events of the same type.

Acknowledgments. MMH is supported by an appointment to the NASA Postdoctoral Program at Goddard Space Flight Center, administered by Oak Ridge Associated Universities through a contract with NASA. The authors thank NASA's MAP program for funding.

REFERENCES

- Adler, R. F., and Coauthors, 2003: The version-2 Global Precipitation Climatology Project (GPCP) monthly precipitation analysis (1979–present). *J. Hydrometeorol.*, **4**, 1147–1167.
- Ashok, K., S. K. Behera, S. A. Rao, H. Weng, and T. Yamagata, 2007: El Niño Modoki and its possible teleconnection. *J. Geophys. Res.*, **112**, C11007, doi:10.1029/2006JC003798.
- Austin, J., and Coauthors, 2003: Uncertainties and assessments of chemistry–climate models of the stratosphere. *Atmos. Chem. Phys.*, **3**, 1–27.
- Bolvin, D. T., R. F. Adler, G. J. Huffman, E. J. Nelkin, and J. P. Poutiainen, 2009: Comparison of GPCP monthly and daily precipitation estimates with high-latitude gauge observations. *J. Appl. Meteor. Climatol.*, **48**, 1843–1857.
- Bosilovich, M., 2008: NASA's Modern Era Retrospective–Analysis for Research and Applications: Integrating earth observations. *Earthzine*, September 26. [Available online at <http://www.earthzine.org/2008/09/26/nasas-modern-era-retrospective-analysis/>.]
- Bronnimann, S., 2007: The impact of El Niño–Southern Oscillation on European climate. *Rev. Geophys.*, **45**, RG3003, doi:10.1029/2006RG000199.
- , J. Luterbacher, J. Staehelin, T. M. Svendby, G. Hansen, and T. Svenoe, 2004: Extreme climate of the global troposphere and stratosphere in 1940–42 related to El Niño. *Nature*, **431**, 971–974, doi:10.1038/nature02982.
- Cagnazzo, C., and Coauthors, 2009: Northern winter stratospheric temperature and ozone response to ENSO inferred from an ensemble of chemistry climate models. *Atmos. Chem. Phys.*, **9**, 8935–8948.
- Calvo, N., R. R. Garcia, W. J. Randel, and D. R. Marsh, 2010: Dynamical mechanism for the increase in tropical upwelling in the lowermost tropical stratosphere during warm ENSO events. *J. Atmos. Sci.*, **67**, 2331–2340.
- Calvo Fernandez, N., R. R. García, R. García Herrera, D. Gallego Puyol, L. Gimeno Presa, E. Hernandez Martín, and P. Ribera Rodríguez, 2004: Analysis of the ENSO signal in tropospheric and stratospheric temperatures observed by MSU, 1979–2000. *J. Climate*, **17**, 3934–3946.
- Collimore, C. C., D. W. Martin, M. H. Hitchman, A. Huesman, and D. E. Waliser, 2003: On the relationship between the QBO and tropical deep convection. *J. Climate*, **16**, 2552–2568.
- Eyring, V., and Coauthors, 2006: Assessment of temperature, trace species and ozone in chemistry–climate model simulations of the recent past. *J. Geophys. Res.*, **111**, D22308, doi:10.1029/2006JD007327.
- Free, M., and D. J. Seidel, 2009: Observed El Niño–Southern Oscillation temperature signal in the stratosphere. *J. Geophys. Res.*, **114**, D23108, doi:10.1029/2009JD012420.
- García-Herrera, R., N. Calvo, R. R. Garcia, and M. A. Giorgetta, 2006: Propagation of ENSO temperature signals into the middle atmosphere: A comparison of two general circulation models and ERA-40 reanalysis data. *J. Geophys. Res.*, **111**, D06101, doi:10.1029/2005JD006061.
- Garfinkel, C. I., and D. L. Hartmann, 2007: Effects of the El Niño–Southern Oscillation and the quasi-biennial oscillation on polar temperatures in the stratosphere. *J. Geophys. Res.*, **112**, D19112, doi:10.1029/2007JD008481.
- , and —, 2008: Different ENSO teleconnections and their effects on the stratospheric polar vortex. *J. Geophys. Res.*, **113**, D18114, doi:10.1029/2008JD009920.
- Holton, J. R., and H.-C. Tan, 1980: The influence of the equatorial quasi-biennial oscillation on the global circulation at 50 mb. *J. Atmos. Sci.*, **37**, 2200–2208.
- Hurwitz, M. M., P. A. Newman, F. Li, L. D. Oman, O. Morgenstern, P. Braesicke, and J. A. Pyle, 2010: Assessment of the breakup of the Antarctic polar vortex in two new chemistry–climate models. *J. Geophys. Res.*, **115**, D07105, doi:10.1029/2009JD012788.
- Juillet-Leclerc, A., S. Thiria, P. Naveau, T. Delcroix, N. Le Bec, D. Blamart, and T. Corrège, 2006: SPCZ migration and ENSO events during the 20th century as revealed by climate proxies from a Fiji coral. *Geophys. Res. Lett.*, **33**, L17710, doi:10.1029/2006GL025950.
- Kanamitsu, M., W. Ebisuzaki, J. Woollen, S.-K. Yang, J. J. Hnilo, M. Fiorino, and G. L. Potter, 2002: NCEP–DOE AMIP-II Reanalysis (R-2). *Bull. Amer. Meteor. Soc.*, **83**, 1631–1643.
- Kug, J.-S., F.-F. Jin, and S.-I. An, 2009: Two types of El Niño events: Cold tongue El Niño and warm pool El Niño. *J. Climate*, **22**, 1499–1515.
- Larkin, N. K., and D. E. Harrison, 2005: On the definition of El Niño and associated seasonal average U.S. weather anomalies. *Geophys. Res. Lett.*, **32**, L13705, doi:10.1029/2005GL022738.
- Manzini, E., M. A. Giorgetta, M. Esch, L. Kornbluh, and E. Roeckner, 2006: The influence of sea surface temperatures on the northern winter stratosphere: Ensemble simulations with the MAECHAM5 model. *J. Climate*, **19**, 3863–3881.
- Newman, P. A., E. R. Nash, and J. E. Rosenfield, 2001: What controls the temperature of the Arctic stratosphere during the spring? *J. Geophys. Res.*, **106** (D17), 19 999–20 010.
- Randel, W. J., R. R. Garcia, N. Calvo, and D. Marsh, 2009: ENSO influence on zonal mean temperature and ozone in the tropical lower stratosphere. *Geophys. Res. Lett.*, **36**, L15822, doi:10.1029/2009GL039343.
- Rasmusson, E. M., and T. H. Carpenter, 1982: Variation in tropical sea surface temperature and surface wind fields associated with Southern Oscillation/El Niño. *Mon. Wea. Rev.*, **110**, 354–384.
- Rayner, N. A., D. E. Parker, E. B. Horton, C. K. Folland, L. V. Alexander, D. P. Rowell, E. C. Kent, and A. Kaplan, 2003: Global analyses of sea surface temperature, sea ice, and night marine air temperature since the late nineteenth century. *J. Geophys. Res.*, **108**, 4407, doi:10.1029/2002JD002670.
- Sassi, F., D. Kinnison, B. A. Boville, R. R. Garcia, and R. Roble, 2004: Effect of El Niño–Southern Oscillation on the dynamical, thermal, and chemical structure of the middle atmosphere. *J. Geophys. Res.*, **109**, D17108, doi:10.1029/2003JD004434.

- Taguchi, M., 2010: Wave driving in the tropical lower stratosphere as simulated by WACCM. Part II: ENSO-induced changes for northern winter. *J. Atmos. Sci.*, **67**, 543–555.
- Uppala, S. M., and Coauthors, 2005: The ERA-40 Re-Analysis. *Quart. J. Roy. Meteor. Soc.*, **131**, 2961–3012, doi:10.1256/qj.04.176.
- Vera, C., G. Silvestri, V. Barros, and A. Carril, 2004: Differences in El Niño response over the Southern Hemisphere. *J. Climate*, **17**, 1741–1753.
- Xie, S.-P., C. Deser, G. A. Vecchi, J. Ma, H. Y. Teng, and A. T. Wittenberg, 2010: Global warming pattern formation: Sea surface temperature and rainfall. *J. Climate*, **23**, 966–986.
- Yeh, S.-W., B. Y. Yim, Y. Noh, and B. Dewitte, 2009: Changes in mixed layer depth under climate change projections in two CGCMs. *Climate Dyn.*, **33**, 199–213.
- Yu, J.-Y., and S. T. Kim, 2010: Three evolution patterns of Central-Pacific El Niño. *Geophys. Res. Lett.*, **37**, L08706, doi:10.1029/2010GL042810.